Fast aerodynamic design of a one-stage axial gas turbine in order to produce a 3D geometry ready for optimization

Artur João Carvalho Batista Soares de Figueiredo
joao.carvalho.batista@ist.utl.pt

Instituto Superior Técnico, Lisboa, Portugal

October 2014

The turbine plays a vital role in major industries worldwide, namely in electricity generation and the aerospace industry. The preliminary design phase of a turbine (one of most important phases of the overall design, since it sets the tone for all subsequent design stages and results) is nowadays often carried out by hand. However, in any industry, reducing costs and increasing efficiency are everyday goals. The need for an automatic, fast and reliable way to perform a preliminary design of an axial turbine in order to produce a 3D geometry ready for optimization brings us to the purpose of this thesis.

The necessary tools for such a preliminary design are nowadays accepted knowledge for any turbine designer. The purpose of this work is to use this knowledge for the creation of a methodology, coded into a *C* program, capable of delivering a feasible and realistic turbine preliminary design ready for optimization, starting only with data from the engine this turbine belongs to.

Typical thermodynamic analysis of an engine (turboshaft), followed by the application of mean line analysis and radial equilibrium theory (ISRE and NISRE) and subsequent airfoil selection compose the main tools in this design. Loss calculation is included with Soderberg's correlation in the 1D design (MLA), and with Craig & Cox's method in the 2D design (RET).

The objective of this thesis was therefore attained, with the development of a methodology able to deliver a full 2D design of a turbine and consequently a 3D geometry.
Keywords: turbine design, preliminary, MLA, RET, airfoil.

Acronyms

Symbol	*Description*
ECA	Engine Cycle Analysis
ISRE	Isentropic Simple Radial Equilibrium
MLA	Mean Line Analysis
NISRE	Non-Isentropic Simple Radial Equilibrium
RET	Radial Equilibrium Theory

Introduction

The understanding of design strategies concerning gas turbines is of utmost importance for a constantly changing and demanding World, where providing a customer with fast and positive answers is a requirement for success, as well as a task of science.

The objective of this thesis is to develop a program that allows a user to obtain a gas turbine 3D geometry ready for optimization, starting from global data.

Therefore, the main goals of this thesis concern the understanding of the engine cycle analysis and the mean line analysis (1D design), including the influence of each variable on feasibility and output power; the understanding of radial equilibrium theory (2D design) and its application in order to obtain a good radial design of the turbine in study; and the understanding of the process of airfoil choosing (3D geometry). In fact, contained in the items previously presented, is also the study of historical trends and good practices of turbine design, knowledge that will be passed to the *C* program developed during this thesis, along with different models for loss calculation in a turbine.

Design Procedure

This design task can be divided in six fundamental elements: the Engine Cycle Analysis, that regards the engine as a whole and takes each element of it as a "black-box"; the Mean Line Analysis, comprising the 1D design of the turbine that is the center of our study; the Design Control, with the purpose of checking the feasibility of the design; the ISRE, Isentropic Simple Radial Equilibrium, a more detailed, 2D analysis of the turbine; the NISRE, Non-Isentropic Simple Radial Equilibrium, which accounts with the losses in this 2D design; and finally the Airfoil Selection, which is based on the results from the NISRE and yields a 3D geometry. The program structure is presented in figure 1 in a flow chart.

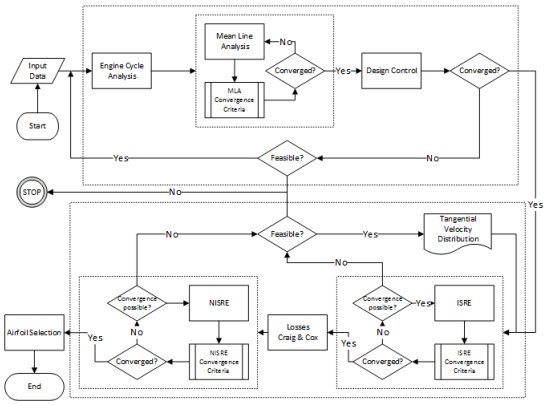

Figure 1: *Design Procedure*

Theoretical Background

Turbine h-s diagram

A complete h-s diagram of a turbine, taken from reference [2], is presented below. This diagram will be used as a reference throughout the entire document for the design and analysis of the turbine.

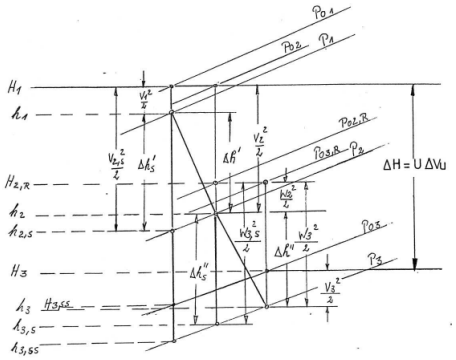

Figure 2: *Typical h-s diagram for a turbine*

Blade Geometry

The following nomenclature is used concerning blade geometry: c is the chord, c_x is the axial chord, g is the pitch, o is the throat, γ is the stagger angle, e is the back surface radius, b is the backbone length and t_e is the trailing edge thickness.

Turbine Velocity Triangles

It is important to refer the different conventions regarding angles and velocities. First, there are different conventions as to whether the angles should be measured from the axial line or the meridional line. Hence forth, these conventions shall be referred to as English and German conventions, respectively. This document takes the English convention as default. However, due to the different references used throughout the document, there may be a need to use the German convention at certain sections of this thesis. In these situations, the read will be informed. The second convention to be discussed regards which is the positive direction of the meridional axis of the reference frame. In this document, and along with the figure above from [3], absolute and relative angles, along with tangential velocities, are measured as positive in the direction of rotation when downstream of the stator. Downstream of the rotor, these quantities are measured as positive against the direction of rotation. However, in many documents, absolute and relative angles, along with tangential velocities, are measured as positive in the direction of rotation when downstream of the rotor. When needed be, the convention may be changed in order to use certain references. Again, the reader will be warned if such is the case.

Adiabatic Flow

When referring to the stator, this simply implies the conservation of total enthalpy, or, since this document always assumes constant c_p, conservation of total temperature. This results in:

$$T_1 + \frac{V_1^2}{2c_p} = T_2 + \frac{V_2^2}{2c_p} \tag{1}$$

It can be shown that, in the the rotor case, rothalpy, I, is conserved: $I = h_0 - UV_\theta$. This results in:

$$T_2 + \frac{W_2^2}{2c_p} - \frac{U_2^2}{2c_p} = T_3 + \frac{W_3^2}{2c_p} - \frac{U_3^2}{2c_p} \tag{2}$$

Turbine Efficiency

Stage Efficiency

The total to total efficiency, used in this document as the main reference for stage efficiency calculation is given by (with a constant c_p):

$$\eta_{TT} = \frac{h_{01} - h_{03}}{h_{01} - h_{03_{ss}}} \tag{3}$$

Blading efficiency

The isentropic blading efficiency definition used as a main reference is, in the stator case:

$$\eta = \frac{h_{01} - h_2}{h_{01} - h_{2_s}} = \frac{T_{01} - T_2}{T_{01} - T_{2_s}} = \frac{V_2^2}{V_{2_s}^2} \tag{4}$$

The loss in kinetic energy definition here used is:

$$\xi = \frac{V_{2_s}^2 - V_2^2}{V_2^2} \tag{5}$$

For the rotor the expressions are similar but using the relative exit velocity of the rotor, W_3.

Radial Equilibrium Theory

In RET we assume that the flow is axisymmetric, the blade rows do not interact and there are no side forces. The basic assumption of radial equilibrium theory is that the radial velocity is zero, $V_r = 0$. Taking the momentum equations of the turbine, according to [3], we arrive at

$$\frac{dh_0}{dr} - \frac{Tds}{dr} = \frac{V_\theta^2}{r} + V_\theta \frac{dV_\theta}{dr} + V_x \frac{dV_x}{dr} \tag{6}$$

For a design exercise one usually takes the total enthalpy as constant, as has been done in this document. The following equation shall be used for the ISRE and NISRE computations.

$$\frac{V_\theta}{r}\frac{d\left(rV_\theta\right)}{dr} + V_x\frac{dV_x}{dr} + T\frac{ds}{dr} = 0 \tag{7}$$

Engine Cycle Analysis

Engine Architecture

The considered engine is a turboshaft engine, comprising a propeller driven by a turbine which shall be mentioned to as power turbine; a compressor driven by another turbine which will be referred to as gas generator (and it is the object of our study) and a combustion chamber. Figure 3 shows a schematic view of the engine and its components, as well as the numbering adopted in order to analyse the engine cycle.

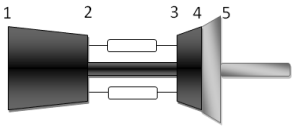

Figure 3: *Engine Scheme*

Global Starting Data

It is observable that several scalars are required as the global starting data. These are: the total pressure at the beginning and end of the cycle, the inlet total temperature, the turbine inlet total temperature, the power required for the power turbine, the pressure ratio achievable by the compressor and the heat capacity ratio and heat capacity at constant pressure for the flows before and after the combustion chamber. Guesses concerning efficiencies of the components, Π_{cc} and LHV are also needed.

Calculation Procedure

The equations here described show the mathematical procedure followed at each iteration of the engine cycle. We note that η_{gg} (the total to total efficiency η_{TT} of the turbine being designed) is, in the first iteration, just a user guess, but shall change according to Soderberg's loss correlation, as will be explained later.

$$T_{02} = T_{01}\left(1 + \frac{1}{\eta_c}\left(\Pi_c^{\frac{\kappa_{air}-1}{\kappa_{air}}} - 1\right)\right) \tag{8}$$

$$p_{02} = \Pi_c p_{01} \tag{9}$$

$$\frac{P_c}{\dot{m}_{air}} = C_{p_{air}}\left(T_{02} - T_{01}\right) \tag{10}$$

$$p_{03} = \Pi_{cc} p_{02} \tag{11}$$

$$\frac{\dot{m}_f}{\dot{m_{air}}} = \frac{C_{p_{gas}}\left(T_{03} - T_{02}\right)}{LHV\eta_{cc} - C_{p_{gas}}\left(T_{03} - T_{02}\right)} \tag{12}$$

$$\frac{P_{gg}}{\dot{m}_{air}} = \frac{\frac{P_c}{\dot{m}_{air}}}{\eta_m} \tag{13}$$

$$T_{04} = \frac{\left(1 + \frac{\dot{m}_f}{\dot{m}_{air}}\right)C_{p_{gas}}T_{03} - \frac{P_{gg}}{\dot{m}_{air}}}{\left(1 + \frac{\dot{m}_f}{\dot{m}_{air}}\right)C_{p_{gas}}} \tag{14}$$

$$p_{04} = \left(1 - \frac{1}{\eta_{gg}}\left(1 - \frac{T_{04}}{T_{03}}\right)\right)^{\frac{\kappa_{gas}}{\kappa_{gas}-1}} p_{03} \tag{15}$$

$$T_{05} = T_{04}\left(1 + \eta_{pt}\left(\frac{p_{05}}{p_{04}}\right)^{\frac{\kappa_{gas}-1}{\kappa_{gas}}-1}\right) \tag{16}$$

$$\dot{m}_{air} = \frac{P_{pt}}{\left(1 + \frac{\dot{m}_f}{\dot{m}_{air}}\right)C_{p_{gas}}\left(T_{04} - T_{05}\right)} \tag{17}$$

$\dot{m}_f$, P_{gg} and P_c follow.

Mean Line Analysis

As a first approach to the actual turbine design we use the mean line analysis, a 1D approach. In this analysis, an imaginary blade-to-blade plane, tangential at the mean radius is analysed and considered representative of the rest of the turbine (a very reasonable assumption for stages where hub and tip speeds are very similar). By applying this approximation, we are able to obtain an averaged analysis of the turbine, therefore allowing a basis to start more complex analysis.

The mean line analysis computes not only the properties of the flow, pressure, temperature, Mach number, but also the velocity triangles of the turbine at mean radius. In fact, losses are also considered, with focus on the efficiencies of the stator and rotor (for now guessed values that must be checked in the end and iterated on).

Losses

Previous Considerations

We must note that the loss calculation occurs at the end of each MLA iteration, when certain quantities are already known, enabling us to calculate the geometry figures that are to follow.

Based on historic trends, we typically assume (this can be changed by the user): $\frac{r_2^h}{r_2^t} = 0.9$, allowing the calculation of stator radii. For the rotor exit radii calculation, the user can choose between two possibilities: to keep the tip radius constant, or to keep the mean radius constant. This defines all the radii of the turbine stage.

The chord is taken as constant from hub to tip, and it's calculated using the height of the blade and typical height to chord ratios. For the stator we typically have $\frac{h}{c} = 0.5 \rightarrow 0.8$ and for the rotor $\frac{h}{c} = 1.1 \rightarrow 1.5$. Values of 0.65 and 1.15 are assumed as default.

The stagger angle prediction is based on the work of KACKER, S.C. and OKAPUU, U. in [4].

The trailing edge thickness is also assumed constant throughout the radius. There are two types of trailing edges to be considered: uncooled(0.5 mm) and cooled (1.2 mm). We now present the flowchart (figure 4) for the calculation of the number of blades, pitch to chord ratio and trailing edge thickness.

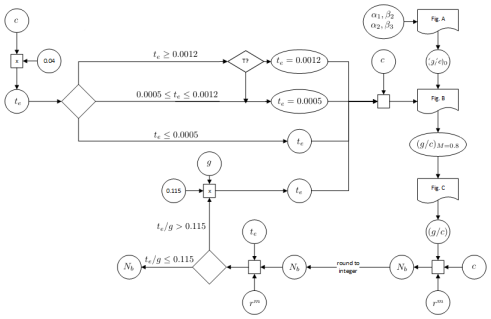

Figure 4: *Flow chart for the calculation of the number of blades*

Figures A B and C referred in the previous flowchart are based on the work of Dejc and Trojanovskij in [5]. This method allows for the calculation of the pitch based on historic trends.

Soderberg's Correlation

Soderberg's correlation is a method for obtaining the losses that is based on the space-chord ratio, Reynolds number, aspect ratio (based on axial chord), thickness ratio and blading geometry. The method is composed of a nominal loss and two corrections, one for the aspect ratio and another for the Reynolds number. The nominal loss is given by figure 5.

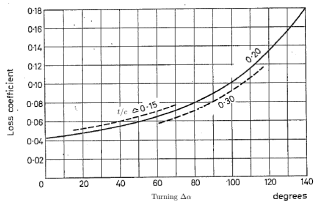

Figure 5: *Soderberg's nominal loss coefficient* $\xi^{'}$

The thickness to chord ratio shown as label for the different carpet plots is neglected. At this stage of the design, we simply take the middle curve as reference for this 1D analysis. The correction for the aspect ratio (based on axial chord) follows.

$$\xi^{''} = \left(1 + \xi^{'}\right)\left(0.975 + 0.075\frac{c_x}{h}\right) - 1 \tag{18}$$

[6] suggests that the expression above is valid for rotors, whilst for stator a small correction must be introduced, resulting in the expression below.

$$\xi^{''} = \left(1 + \xi^{'}\right)\left(0.993 + 0.075\frac{c_x}{h}\right) - 1 \tag{19}$$

The last correction concerns the Reynolds number (based on the hydraulic diameter Dh).

$$\xi^{'''} = \left(\frac{10^5}{Re_{Dh}}\right)^{1/4} \xi^{''} \tag{20}$$

Calculation Procedure

This computation is an iterative process. A value for M_3 is guessed at the beginning of the computation. In the end, a new value for M_3 is found and the cycle restarts until convergence. Several choices and guesses are used along the way (β_3, U, α_2, R_p, η_S, η_R, M_3). For the sake of simplicity, in the first approach implemented, the choices made throughout the cycle deliver a turbine with the minimum possible exit Mach number, which translates into a higher efficiency. The implemented cycle is now presented. By knowing the guessed value of M_3, we have:

$$p_3 = p_{03}\left(1 + \frac{\kappa - 1}{2}M_3^2\right)^{\frac{-\kappa}{\kappa-1}} \tag{21}$$

$$T_3 = T_{03}\left(1 + \frac{\kappa - 1}{2}M_3^2\right)^{-1} \tag{22}$$

$$p_2 = R_p\left(p_1 - p_3\right) + p_3 \tag{23}$$

In the first iteration p_1 is unknown. Hence, as a first guess, p_{01} is used instead.

$$M_{2_s} = \sqrt{\frac{2}{\kappa - 1}\left(\left(\frac{p_2}{p_{01}}\right)^{\frac{-\kappa}{\kappa-1}} - 1\right)} \tag{24}$$

$$T_{2_s} = T_{01}\left(1 + \frac{\kappa - 1}{2}M_{2_s}^2\right)^{-1} \tag{25}$$

$$V_{2_s} = M_{2_s}\sqrt{\kappa R T_{2_s}} \tag{26}$$

$$V_2 = V_{2_s}\sqrt{\eta_S} \tag{27}$$

$$T_2 = T_{01} - \frac{V_2^2}{2c_p} \tag{28}$$

$$V_2\cos\left(\alpha_2\right) = W_2\cos\left(\beta_2\right) \tag{29a}$$

$$V_2\sin\left(\alpha_2\right) = U + W_2\sin\left(\beta_2\right) \tag{29b}$$

Since we know V_2, α_2 and U, W_2 and β_2 follow from the two equations above.

$$T_{3_s} = T_2\left(\frac{p_3}{p_2}\right)^{\frac{k-1}{k}} \tag{30}$$

$$T_2 + \frac{W_2^2}{2c_p} = T_{3_s} + \frac{W_{3_s}^2}{2c_p} \tag{31}$$

$$W_3 = W_{3_s}\sqrt{\eta_R} \tag{32}$$

$$V_{3_\theta} = W_3\sin\left(\beta_3\right) - U \tag{33}$$

$$P_{av} = \dot{m}U\left(V_{2_\theta} + V_{3_\theta}\right) \tag{34}$$

In order to reach convergence, we calculate M_3 at the end of this procedure and feed it back to the beginning of the cycle. At this point, after the iteration on M_3, we are able to compute the initial conditions, that is, the conditions on the stator inlet. We first take the mass flow equation for section 1 and we assume the flow fully axial ($V_{1_x} = V_1$). By taking the relation between total temperature, temperature and velocity we can write:

$$V_1 = \sqrt{\left(2c_pT_{01}\left(1 - \frac{T_1}{T_{01}}\right)\right)} = \sqrt{\left(2c_pT_{01}\left(1 - \left(\frac{\rho_1}{\rho_{01}}\right)^{\kappa-1}\right)\right)} \tag{35}$$

Since we can calculate ρ_{01} with $\rho_{01} = \frac{p_{01}}{RT_{01}}$, we can discover ρ_1 by iteration. Therefore, V_1, T_1 and p_1 can be calculated. We can go back to the calculation with a new initial guess of p_1 to use in equation 23. Every time a new value of p_1 is fed back to the beginning of the cycle, the iteration on M_3 must occur again.

At the end of the iteration on p_1, the losses are calculated using Soderberg's correlation, allowing us to find new values to feed back to the beginning of the cycle. Again, every time this happens, until convergence on the losses, new iterations on p_1 must occur, along with the consequent iterations on M_3.

Design Veracity, Control and Optimization

Total to Total Efficiency Convergence

Taking into account figure 2 and assuming that we have a negligible divergence between the p_2 and p_3 isobars we can assume that the total enthalpy loss is equal to the sum of the enthalpy losses in stator and rotor $((h_{03} - h_{03_{ss}}) = (h_3 - h_{3_s}) + (h_2 - h_{2_s}))$. Therefore, it can be demonstrated that:

$$\eta_{TT} = \frac{1}{1 + \frac{\xi_S \frac{V_2^2}{2} + \xi_R \frac{W_3^2}{2}}{h_{01} - h_{03}}} \tag{36}$$

Therefore, at the end of the mean line analysis, we have a new value for the parameter η_{TT} (η_{gg} in the ECA) that was given as a guess to the engine cycle analysis, thus allowing us to iterate between the ECA and the MLA.

Exit Mach Number Optimization

It is observable that the general trends in the variables that allow for a smallest as possible exit Mach number are (within user given limits): R_p as low as possible, α_2 as high as possible, U as high as possible and β_3 as high as possible. These are only general individual trends of these variables.

The initial guess for U is changed, using the values for the radius calculated at each iteration, until the program arrives at a $U^t \approx 500$ m/s, highest possible value due to material limitations. The other variables, R_p, α_2 and β_3 are subject to change only if really necessary for the purpose of power or design control.

Power Availability

The power delivered by the turbine was calculated in different ways in the engine cycle analysis and the mean line analysis.

Given that the total to total efficiency is being iterated on until convergence, it is expected that the power delivered is the same independently of the formula. Since the convergence is never perfect however, small changes may arise. Also, the values imposed to design variables such as α_2 or β_3 may not be able to deliver a turbine with the desired power.

Hence, in the case that $P_{MLA} < P_{ECA}$ the following action is taken, in order of desirability, according to whatever can help in minimizing M_3 or at least harm this minimization the least (second and third choices are only activated if the previous choice is no longer possible due to imposed variable limits): 1) increase α_2; decrease R; increase β_3.

Design Control

This control is mostly based on guide lines given in [2], along with suggested actions if the design does not comply.

1. $0.85 < M_2 < 1.2$: increase R if $M_2 > 1.2$ and decrease R if $M_2 < 0.85$;
2. $\beta_2 < 45^\circ$ or $M_2^r < 0.5$: 1) decrease α_2; 2) increase R;
3. $\beta_2 + \beta_3 < 110^\circ$: 1) decrease α_2; 2) increase R; 3) decrease β_3;
4. $0.85 < M_3^r < 1.3$: if $M_3^r < 0.85$ increase $R(1)$ and decrease $\beta_3(2)$; if $M_3^r > 1.3$ decrease $R(1)$ and increase $\beta_3(2)$;
5. $h_3/h_2 < 1.2$: 1)increase α_2; 2) decrease β_3;
6. $\alpha_3 < 30^\circ$: decrease β_3;

It may happen that two requirements may demand counter-actions. If so, when finding a counter-action, the program tries using secondary options in order to satisfy both requirements.

Radial Equilibrium

ISRE

We start by taking equation 7 and assuming isentropic behaviour, $\frac{ds}{dr} = 0$. We observe that by admitting a certain tangential velocity distribution, we can compute the axial velocity. The general distribution equation is given by:

$$V_\theta = Ar^n \pm \frac{B}{r} \tag{37}$$

The plus sign corresponds to the flow downstream of the rotor and the minus sign corresponds to the flow upstream of the rotor. The three different cases programmed are presented below, with expressions for the tangential and axial velocity distributions. An important note regarding the equation above is that it is written considering the direction of the axis as positive in the direction of rotation when downstream of the rotor. This goes against the convention used in this document. However, for the sake of uniformity with most documents regarding this subject, the expressions are kept for this part of the calculation only. In the end, the results are translated to the convention used in the document, so that they can be used for other sections of the design exercise.

Vortex Design In Free Vortex Design we have:

$$V_\theta = \frac{B}{r} \tag{38}$$

We can determine B (different for the stator and for the rotor) using $V_\theta^m = \frac{B}{r^m}$. Therefore, in Free Vortex design,

$$V_x = const. \tag{39}$$

Constant Degree of Reaction Design

$$V_\theta = Ar \pm \frac{B}{r} \tag{40}$$

Since we know that A and B must be the same in front and behind the rotor, we can use mean line analysis data to find these constants (the same will be done for the exponential design). This leads to:

$$V_{2_x} = \sqrt{-2A^2\left(r_2^2 - r_2^{m2}\right) + 4AB\ln\left(\frac{r_2}{r_2^m}\right) + V_{2_x}^{m2}} \tag{41a}$$

$$V_{3_x} = \sqrt{-2A^2\left(r_3^2 - r_3^{m2}\right) - 4AB\ln\left(\frac{r_3}{r_3^m}\right) + V_{3_x}^{m2}} \tag{41b}$$

Exponential Design

$$V_\theta = A \pm \frac{B}{r} \tag{42}$$

$$V_{2_x} = \sqrt{-2A^2\ln\left(\frac{r_2}{r_2^m}\right) - 2AB\left(\frac{1}{r_2} - \frac{1}{r_2^m}\right) + V_{2_x}^{m2}} \tag{43a}$$

$$V_{3_x} = \sqrt{-2A^2\ln\left(\frac{r_3}{r_3^m}\right) + 2AB\left(\frac{1}{r_3} - \frac{1}{r_3^m}\right) + V_{3_x}^{m2}} \tag{43b}$$

Calculation Procedure

The iterative process applied for the ISRE will now be presented. A first initial guess of V_x^m is taken. As such, using the constants previously computed and this initial guess, we can compute the entire velocity distribution for any given radius. The iterative cycle is composed of 4 main equations, all dependent on the radius through the expressions of the tangential and axial velocity. These 4 equations are now presented.

$$T_2(r_2) = T_{01} - \frac{1}{2c_p}\left(V_{2_x}^2(r_2) + V_{2_\theta}^2(r_2)\right) \tag{44a}$$

$$p_2(r_2) = p_{01}\left(\frac{T_2(r_2)}{T_{01}}\right)^{\frac{\kappa}{\kappa-1}} \tag{44b}$$

$$\rho_2(r_2) = \frac{p_2(r_2)}{RT_2(r_2)} \tag{44c}$$

$$\dot{m} = \int_{r_2^h}^{r_2^t} 2\pi r_2 \rho_2(r_2) V_{2_x}(r_2) dr \tag{44d}$$

We remark the important detail of equation 44b using p_{01} ($p_{02}^r(r_2)$ in equation 45c), representing the non-existence of losses in this computation, and the use of T_{01} in equation 44a ($T_{03}^r(r_3)$ in equation 45b), which translates as adiabatic flow. After performing this calculation for the stator, we are able to calculate p_{02}^r and T_{02}^r, which will be used for the same type of computation for the rotor, as described below. In fact, relative quantities are used for the rotor calculation.

$$W_{3_\theta}(r_3) = V_{3_\theta}(r_3) + \Omega r_3 \tag{45a}$$

$$T_3(r_3) = T_{03}^r(r_3) - \frac{1}{2c_p}\left(W_{3_x}^2(r_3) + W_{3_\theta}^2(r_3)\right) \tag{45b}$$

$$p_3(r_3) = p_{02}^r(r_3)\left(\frac{T_3(r_3)}{T_{03}^r(r_3)}\right)^{\frac{\kappa}{\kappa-1}} \tag{45c}$$

$$\rho_3(r_3) = \frac{p_3(r_3)}{RT_3(r_3)} \tag{45d}$$

$$\dot{m} = \int_{r_3^h}^{r_3^t} 2\pi r_3 \rho_3(r_3) V_{3_x}(r_3) dr \tag{45e}$$

These integrals were performed in 20 sections along the radius. In the end, the value obtained for $\dot{m}$ is compared to the one calculated in the engine cycle analysis. The initial guess of V_x^m is changed accordingly, until convergence. All distributions of temperature and pressure, both static and total, absolute and relative, along with velocity, Mach number, angles and enthalpy degree of reaction are computed for all sections of the turbine.

Losses

This loss section is mainly based on reference [7]. The losses can be divided into the following types: profile losses, secondary losses, annulus losses and leakage losses. It is important to notice though, that these coefficients, as calculated in [7], must be summed, according to whichever distribution they have (for example the leakage losses will only occur at the tip). X, the total loss calculated from [7] corresponds to the loss in kinetic energy referred to the real velocity, as presented in equation 5.

Previous Considerations

Some aspects of the turbine geometry must be computed before starting the losses calculation, including an update of the quantities referred before in the MLA. Also, the angles definition used in [7] is different from the one used in this document. These are measured from the meridional line. For simplicity, in this section, whenever any angle is referred to, it corresponds to the definition in [7] (German convention). All geometry previously calculated is reviewed at this point of the calculation.

Profile Losses

The profile losses are the losses related to the friction on the blade profiles and also to the blade wakes. For the profile loss calculation, the incidence angles are supposed to be zero and the blades are assumed straight backed blades, since this will lead to smaller profile losses. For each radial position, the following quantities are computed: pitch; pitch over backbone length ($\frac{g}{b} = \frac{\frac{g}{c}}{0.72+0.005\Delta\alpha}$); throat size (based on the sine-rule for the outlet angle); and Reynolds number based on the throat size. Sutherland's Law was used in order to calculate the dynamic viscosity. We are now able to use the plots from [7] in order to calculate the profile losses. The profile loss factor in the correlation proposed in [7] is given by the following equation.

$$X_p = x_{pb} N_{pr} N_{pt} + (\Delta x_p)_t + (\Delta x_p)_m \tag{46}$$

N_{pr} presents the effect of the Reynolds number on the profile loss ratio, x_{pb} is the basic profile loss parameter, N_{pt} gives a correction on the profile loss ratio based on the trailing edge thickness over pitch ratio, $(\Delta x_p)_t$ is a further increment on the profile losses based on the trailing edge thickness over pitch ratio and finally $(\Delta x_p)_m$ is yet another increment, to account for Mach number effects.

N_{pr} is based on a plot that depends on the smoothness of the blades. A standard finish is assumed, which corresponds to the value of 0.1. The plots used for this calculation are available in reference [7].

Secondary Losses

The secondary losses are the losses related to the friction on the walls at root and tip, together with any other end effects. Given this, it is obvious that secondary losses occur mainly at the hub and tip and seldomly at mean radius. Instead of calculating the losses for several lines parallel to the walls, we actually get only two values from [7], using hub and tip radii values. Each of these values represents an overall integrated value of the secondary losses. The reason for the calculation of two values, one at hub and another at tip, instead of only one at the mean radius, lies with the possible asymmetry in the secondary losses distribution. Having two values, we are able to ponder on the amount of secondary losses distribution for either hub or tip. After calculated, the secondary losses must be redistributed. First, however, the process for finding a value for the secondary losses from [7] will be explained. All the calculations here presented are performed the same way for stator and rotor. According to [7], the secondary losses are given by:

$$X_s = (N_s)_r (N_s)_{h/b} (x_s)_b \tag{47}$$

$(N_s)_r$ is the same Reynolds number correction used for the profile losses, $(N_p)_r$. The plots for $(N_s)_{h/b}$ (secondary loss ratio against aspect ratio factor) and $(x_s)_b$ (basic secondary loss parameter) are available in reference [7].

We can now proceed to the redistribution of these losses. Two decisions must be made concerning this redistribution. The first is the level of penetration of the secondary losses. This is the percentage of blade height, starting from the walls, that is affected by the secondary loss of each wall. The second decision is the type of distribution of these losses. The secondary losses are higher at the walls and decrease to zero when reaching the point on the radius previously defined with the level of penetration. This variation may be modelled in two ways: with a linear distribution or a parabolic distribution. The integral of these curves inside the radius defined by the level of penetration must be equal to the integral of the average of the values found in [7] using the hub and tip radius values.

As suggested in [8], an averaged value for the secondary losses can be found with a sort of mass averaging of the secondary losses at the hub and tip, hence finding the final value for the secondary losses from the Craig & Cox correlation, $(X_s)_{CC}$.

Level of Penetration [7] does not present any indication concerning this topic. However, Holliger [9], defines a critical aspect ratio (based on pitch), depending on the profile losses, at which the secondary flow regions extend to half the blade height. This correlation, adapted by [2], is given by: $\left(\frac{h}{g}\right)_{cr} = 7 \rightarrow 10\sqrt{\zeta_p}$. Four critical blade heights are computed, for hub and tip of stator and rotor, using the correspondent values at these geometric points for ζ_p(loss of kinetic energy as referred to the isentropic velocity) and g. Since this critical blade height corresponds to secondary flow regions with half the blade height, then we can find the level of penetration through: $p = 0.5\frac{h_{cr}}{h}$. This value may never be above 50%, since it is not physically possible. If the computation delivers such a case, the program assumes a value of 50%.

Linear Distribution We arrive at the following equations for the tip and hub, respectively:

$$X_s^t = \frac{2\,(X_s)_{CC}}{p^t\,(1+K)} \left(\frac{r - r^{t0}}{p^t h}\right) \tag{48a}$$

$$X_s^h = \frac{2K\,(X_s)_{CC}}{p^h\,(1+K)} \left(\frac{r^{h0} - r}{p^h h}\right) \tag{48b}$$

Parabolic Distribution We arrive at the following equations for the tip and hub, respectively:

$$X_s^t = \frac{3\,(X_s)_{CC}}{(1+K)\,p^t} \frac{\left(r - r^{t0}\right)^2}{{p^t}^2 h^2} \tag{49a}$$

$$X_s^h = \frac{3K\,(X_s)_{CC}}{(1+K)\,p^h} \frac{\left(r - r^{h0}\right)^2}{{p^h}^2 h^2} \tag{49b}$$

These equations are only valid for their own domain $\left[r^h, r^{h0}\right]$ and $\left[r^{t0}, r^t\right]$, for the hub and tip, respectively, for both linear and parabolic distributions. This procedure is valid for both stator and rotor.

Annulus Losses

We know from the start that the annulus losses will have a negligible impact on the total losses. Hence, they are not taken into account.

Leakage Losses

Leakage losses can occur over blade tips, around shrouding, through disc balance holes, etc.. The equation below gives the reduction of blading efficiency due to tip clearance losses when compared to the blading efficiency for zero tip clearance, that is, the efficiency calculated before, comprising profile and secondary losses.

$$\Delta\eta_k = F_k \frac{A_k}{A_t} \eta_{\substack{zero \\ clearance}} \tag{50}$$

[7] tells us that this equation must be multiplied by a factor of 1.5 in case of an unshrouded turbine, which we assume to never be the case, in order to have an efficiency as high as possible. The efficiency debit factor F_k is taken from a plot available in reference [7]. ΔL, the tip clearance was defined by the rule of thumb that $\Delta L = 0.007h$. However, this may not be feasible due to machining limitations. Thus, a minimum limit of 0.2 mm was imposed. A_k is the total effective area of clearance whilst A_t is the total blade throat area. We assume the clearance losses affect 30% of the blade height, with higher loss at the tip (the value $\Delta\eta_k$), in a linear distribution until we reach zero at a point 30% of the blade height away from the tip.

NISRE

The NISRE (non-isentropic simple radial equilibrium) takes into account the losses in the turbine. These losses are calculated from [7], as presented before. This results in the following expressions for the axial velocity:

$$\text{Free Vortex Design: } V_{2_x} = \sqrt{V_{2_x}^{m2} - 2\int_{r_2^m}^{r_2} T_2 \frac{ds_S}{dr} dr} \tag{51a}$$

$$\text{Constant DR Design: } V_{2_x} = \sqrt{-2A^2\left(r_2^2 - r_2^{m2}\right) + 4AB\ln\left(\frac{r_2}{r_2^m}\right) - 2\int_{r_2^m}^{r_2} T_2 \frac{ds_S}{dr} dr + V_{2_x}^{m2}} \tag{51b}$$

$$\text{Exponential Design: } V_{2_x} = \sqrt{-2A^2\ln\left(\frac{r_2}{r_2^m}\right) - 2AB\left(\frac{1}{r_2} - \frac{1}{r_2^m}\right) - 2\int_{r_2^m}^{r_2} T_2 \frac{ds_S}{dr} dr + V_{2_x}^{m2}} \tag{51c}$$

$$\text{Free Vortex Design: } V_{3_x} = \sqrt{V_{3_x}^{m2} - 2\int_{r_3^m}^{r_3} T_3 \frac{ds_R}{dr} dr} \tag{51d}$$

$$\text{Constant DR Design: } V_{3_x} = \sqrt{-2A^2\left(r_3^2 - r_3^{m2}\right) - 4AB\ln\left(\frac{r_3}{r_3^m}\right) - 2\int_{r_3^m}^{r_3} T_3 \frac{ds_R}{dr} dr + V_{3_x}^{m2}} \tag{51e}$$

$$\text{Exponential Design: } V_{3_x} = \sqrt{-2A^2\ln\left(\frac{r_3}{r_3^m}\right) + 2AB\left(\frac{1}{r_3} - \frac{1}{r_3^m}\right) - 2\int_{r_3^m}^{r_3} T_3 \frac{ds_R}{dr} dr V_{3_x}^{m2}} \tag{51f}$$

On the other hand, the tangential velocities expressions are the same. For each radial position r, the integral $\int_{r^m}^{r} T\frac{ds}{dr}dr$ must be evaluated carefully. Whereas when we have an $r > r^m$ the integral remains as it is, when $r < r^m$ we must observe that $\int_{r^m}^{r} T\frac{ds}{dr}dr = -\int_{r}^{r^m} T\frac{ds}{dr}dr$. Given the relation between the axial velocity and $T\frac{ds}{dr}$, we must now relate the losses on [7] with $T\frac{ds}{dr}$. The basis for this connection are the expressions below, the total pressure loss coefficient:

$$\text{Stator: } \omega_S = \frac{p_{01} - p_{02}}{\rho_2 \frac{V_2^2}{2}} \tag{52a}$$

$$\text{Rotor: } \omega_R = \frac{p_{02}^r - p_{03}^r}{\rho_3 \frac{W_3^2}{2}} \tag{52b}$$

According to [2], the total pressure loss coefficient is related to the kinetic loss coefficient ξ, that has the same definition as X (from the Craig & Cox correlation), through:

$$\text{Stator: } \omega_S = X_S\left(1 + \kappa\frac{M_2^2}{2}\right) \tag{53a}$$

$$\text{Rotor: } \omega_R = X_R\left(1 + \kappa\frac{\left(M_3^r\right)^2}{2}\right) \tag{53b}$$

Entropy Increase Stator

For each radial position r_2, the increase in entropy can be found at the stator exit using first equation 53a to find ω and then equation 52a to find a new p_{02} distribution. We can hence calculate Δs_S. According to [2] we have,

$$\Delta s_S\left(r_2\right) = -R\ln\left(\frac{p_{02}\left(r_2\right)}{p_{01}}\right) \tag{54}$$

This allows us to compute $\frac{ds}{dr}$.

Calculation Procedure Stator

The NISRE calculation must start with an ISRE calculation. The losses, calculated using [7] follow. The p_0 losses and entropy increase are then calculated for the stator exit, first using ISRE values. At this point we compute $T_2\frac{ds_S}{dr}$, using on the first iteration ISRE values. After this, we find an absolute axial mean velocity at the stator exit that satisfies the mass flow from the engine cycle, with a procedure similar to the one on ISRE. We must iterate on the static temperature between the point of calculation of $T_2\frac{ds_S}{dr}$ and the final results after the mass flow has been satisfied, until convergence. Also, this iterative cycle is inside a bigger iterative cycle starting on the entropy increase. Therefore, these results from the mass flow cycle are also used to be fed back to the entropy increase calculation, until convergence on p_{02}. The equations for the mass flow cycle are reproduced below.

$$T_2(r_2) = T_{01} - \frac{1}{2c_p}\left(V_{2_x}^2(r_2) + V_{2_\theta}^2(r_2)\right) \tag{55a}$$

$$p_2(r_2) = p_{02}(r_2)\left(\frac{T_2(r_2)}{T_{01}}\right)^{\frac{\kappa}{\kappa-1}} \quad (55b)$$

$$\rho_2(r_2) = \frac{p_2(r_2)}{RT_2(r_2)} \quad (55c)$$

$$\dot{m} = \int_{r_2^h}^{r_2^t} 2\pi r_2 \rho_2(r_2) V_{2_x}(r_2) dr \quad (55d)$$

Entropy Increase Rotor

We first calculate p_{02}^r and T_{03}^r using the converged NISRE results of the stator. We are now in position to compute $\frac{ds}{dr}$ for the rotor. Just like in the stator case, we use equation 53b to calculate ω and then 52b in order to compute p_{03}^r.

$$\Delta s_R\,(r_3) = c_p \ln\left(\frac{T_{03}^r(r_3)}{T_{02}^r(r_2)}\right) - R\ln\left(\frac{p_{03}^r\,(r_3)}{p_{02}^r\,(r_2)}\right) \quad (56)$$

We note that the expression for Δs_R depends also on the total relative temperature ratio, unlike in the stator case, since we have $T_{01} = T_{02}$ but $I_2 = I_3$, which results in $T_{02}^r \neq T_{03}^r$.

Calculation Procedure Rotor

The NISRE calculation for the rotor follows the same steps as for the stator. However, relative quantities are used. The iterations are similar: besides the mass flow cycle, we have an iteration on $T_3 \frac{ds_R}{dr}$ and on p_{03}^r.

$$W_{3_\theta}(r_3) = V_{3_\theta}(r_3) + \Omega r_3 \quad (57a)$$

$$T_3(r_3) = T_{03}^r(r) - \frac{1}{2c_p}\left(W_{3_x}^2(r_3) + W_{3_\theta}^2(r_3)\right) \quad (57b)$$

$$p_3(r_3) = p_{03}^r(r_3)\left(\frac{T_3(r_3)}{T_{03}^r(r_3)}\right)^{\frac{\kappa}{\kappa-1}} \quad (57c)$$

$$\rho_3(r_3) = \frac{p_3(r_3)}{RT_3(r_3)} \quad (57d)$$

$$\dot{m} = \int_{r_3^h}^{r_3^t} 2\pi r_3 \rho_3(r_3) V_{3_x}(r_3) dr \quad (57e)$$

The results of the NISRE (new distributions for velocity, temperature, pressure, etc.) are computed after convergence.

Airfoil Selection

After the completion of the NISRE calculation, we proceed to the calculation of the NACA profiles for the turbine. For this purpose, we use the work of James Dunavant and John Erwin [10]. [10] offers two possible profiles. Only the primary airfoil (named A_3K_7), with a maximum thickness over chord at 20% of the chord, was considered for this methodology. The method of construction of the airfoils using these data is presented in figure 6, adapted from [10].

The camber coordinates are given in [10] as a percentage of the chord. The y_c data is given for a $C_{l_0} = 1.0$ (C_{l_0} is the *camber, expressed as design lift coefficient of isolated airfoil*[10]). Calculating x_c for each blade control point i is direct. We must simply compute: $(x_c)_i = x_c \frac{c}{100}$. The chords are the same for the entire vane and blade. Hence, x_c is the same at all control points of stator and rotor.

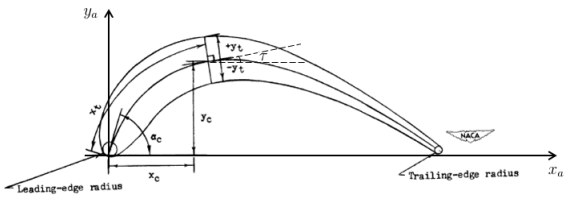

Figure 6: *Method of blade construction*

In what concerns y_c, we can write: $(y_c)_i = (C_{l_0})_i (y_c)_{C_{l_0}=1.0} \frac{c}{100}$. C_{l_0} can be computed knowing the control section turning angle. From [10], we have,

$$(\Delta\alpha)_c = \Delta\alpha + (\Delta\alpha)_{induced} + (\Delta\alpha)_{deviation} = \arctan\left(C_{l_0}\left(\frac{dy_c}{dx_c}\right)_{0.5}\right) - \arctan\left(C_{l_0}\left(\frac{dy_c}{dx_c}\right)_{95}\right) \quad (58)$$

We now can calculate $(\Delta\alpha)_c$ through equation 58 and data given in [10]. Using the right-hand side of this equation we can find C_{l_0} for each control point through an iterative cycle. Finally, we can find $(y_c)_i$ and complete the coordinates that define the camber line. The coordinates for the thickness are given in percentage of the mean line length. The mean line length of an airfoil can be calculated using the coordinates x_c and y_c, with j representing the points that make up the airfoil at the control point i.

$$ml_i = \sum_j \sqrt{\left((x_c)_i^{j+1} - (x_c)_i^j\right)^2 + \left((y_c)_i^{j+1} - (y_c)_i^j\right)^2} \quad (59)$$

Therefore, we can already calculate $(x_t)_i$: $(x_t)_i = x_t \frac{ml_i}{100}$. y_t is tabulated for a thickness over chord of 20%. Hence, in order to achieve other thickness over chord ratios, we must simply multiply by the ratio of the desired thickness to 20%. Therefore, the calculation of y_t for each blade control point i can be summed up in the following fashion: $(y_t)_i = y_t \frac{ml_i}{100} \frac{t/c}{0.2}$. Two more quantities can be calculated for the airfoils according to [10]. The trailing edge radius, TER, which depends only on the chord. Therefore, we will have one value for the stator and another for the rotor. $TER = 0.01c$. The leading edge radius, LER, depends not only on the chord, but also on the mean line length. Hence, we will have different values for each control point at stator and rotor. According to [10], the leading edge radius is given by: $(LER)_i = 0.04407(ml)_i \left(\frac{\frac{t}{c}\frac{c}{(ml)_i}}{20}\right)^2$.

Coordinates in the airfoil reference frame

Using figure 6 we can calculate the coordinates of the upper and lower surfaces of the airfoil. Given that the information for the camber and the one for the thickness are in two different reference frames, we first find a correspondence between the camber coordinates and the thickness coordinates of the airfoil, using equation 59 and figure 6. Given that the thickness is distributed along the camber line on perpendiculars, we must calculate the derivative of the camber line at each point, in order to find the angle τ, shown in figure 6, necessary to calculate the final coordinates. The geometric transformation of the coordinates is given below, as a direct result of figure 6.

$$\begin{bmatrix} x_a^u \\ y_a^u \\ x_a^l \\ y_a^l \end{bmatrix} = \begin{bmatrix} 1 & 0 & -\sin(\tau) \\ 0 & 1 & \cos(\tau) \\ 1 & 0 & \sin(\tau) \\ 0 & 1 & -\cos(\tau) \end{bmatrix} \begin{bmatrix} x_c \\ y_c \\ y_t^n \end{bmatrix} \tag{60}$$

Coordinates in the vane/blade reference frames

The vane/blade coordinates must account with the stagger angle previously calculated. The leading edge is the reference point in this transformation, that is, the only point kept unchanged and common to all airfoils.

$$\text{Stator: } \begin{bmatrix} x \\ \theta \end{bmatrix} = \begin{bmatrix} \cos(\gamma) & \sin(\gamma) \\ \sin(\gamma) & -\cos(\gamma) \end{bmatrix} \begin{bmatrix} x_a \\ y_a \end{bmatrix} \tag{61a}$$

$$\text{Rotor: } \begin{bmatrix} x \\ \theta \end{bmatrix} = \begin{bmatrix} \cos(\gamma) & \sin(\gamma) \\ -\sin(\gamma) & \cos(\gamma) \end{bmatrix} \begin{bmatrix} x_a \\ y_a \end{bmatrix} \tag{61b}$$

Conclusions

A solid knowledge of the design process needed for the preliminary design of a turbine exists. On the other hand, a compilation of this process under an automated program that contains the knowledge necessary for such a design was needed. Hence, the major contribution of this thesis is the program hereby developed, that can obtain a feasible and realistic preliminary design of a turbine through a fast computation process, up to a 3D geometry, including a process of choosing airfoils for different radial control sections.

The results of this program were compared against another program in development at VKI that delivers similar outputs, though with a different calculation process. The results were very comparable, and therefore satisfying, enabling us to trust the results delivered by this program.

The results delivered were also satisfying in the control of design aspect. Upon analysis of the results of the 1D design, the action of the design control is visible, enabling the program to deliver more realistic and feasible results. The 2D design, with three tangential velocity distributions, proved capable of analysing which velocity distributions are feasible or not, and also of restarting the 2D calculation for a new tangential velocity distribution when needed.

Therefore, the objective of this thesis, meeting the need for an automatic, fast and reliable way to perform a preliminary design of a one-stage axial gas turbine turbine in order to produce a 3D geometry ready for optimization, is considered accomplished.

Acknowledgements

The fulfilment of this thesis would have been impossible without the help of many people. Therefore, I must express my thanks: to my supervisor at Von Karman Institute for Fluid Dynamics, Professor Tony Arts; to my supervisor at Instituto Superior Técnico of Lisbon, Professor Afzal Suleman; and to many others who have helped in developing and enriching this Master's Thesis;

To my Mother, Cândida Perpétua Carvalho, for all the help given at all times.

References

[1] *ARTS, T., Private communication, 2014*

[2] *SIEVERDING, C.H., Advanced Course on Turbines, Von Karman Institute for Fluid Dynamics, 2014*

[3] *HORLOCK, J.H., Axial Flow Turbines, Fluid Mechanics and Thermodynamics, Butterworths, 1966*

[4] *KACKER, S.C., OKAPUU, U., A mean line prediction method for axial turbine efficiency, J. Engineering for Power, Vol. 104, 1982*

[5] *DEJC, M.E., TROJANOVSKIJ, B.M, Untersuchung und Berechnung axialer Turbinenstufen, VEB Verlag Berlin1, 1973*

[6] *WEI, N., Significance of Loss Models in Aerothermodynamic Simulation for Axial Turbines, Royal Institute of Technology, 2000*

[7] *CRAIG, H.R.M., COX, H.J.A., Performance Estimation of Axial Flow Turbines, Proceedings of the Institute of Mechanical Engineers, Vol 185, 32, 1970-71*

[8] *TRAUPEL, W., Termische Turbomachinen, Bd. 1: Thermodynamisch-strömungstechnische Berechnung, Springer Verlag Berlin, 1977*

[9] *HOLLIGER, K., Weiterentwicklung von Dampfturbinen-Schaufelungen, Escher Wyss Mitt. 33. Jg., 75-81, 1960*

[10] *DUNAVANT, J., ERWIN, J., Investigation of a Related Series of Turbine-Blade Profiles in Cascade, National Advisory Committee for Aeronautics, December 7, 1953*

[11] *MORAN, M.J., SHAPIRO, H.N., Fundamentals of Engineering Thermodynamics: SI Edition, 6^{th} Edition, John Wiley & Sons, 2009*

[12] *MÜLLER, L., Design Exercise: Cold Rig, Von Karman Institute for Fluid Dynamics, April 2011*